Cellular response of Fusarium oxysporum to crocidolite asbestos as revealed by a combined proteomic approach

M. Chiapello; S. Daghino; E. Martino; S. Perotto
Cellular response of Fusarium oxysporum to crocidolite asbestos as revealed by a combined proteomic approach
JOURNAL OF PROTEOME RESEARCH (2010) 9(8)
DOI: 10.1021/pr100133d

Cellular Response of *Fusarium oxysporum* to Crocidolite Asbestos As Revealed by a Combined Proteomic Approach

Marco Chiapello , Stefania Daghino , Elena Martinoand Silvia Perotto

Synopsis

Cellular mechanisms of asbestos toxicity rely, at least in part, on the chemical composition of these minerals, with iron ions being directly involved. The soil fungus Fusarium oxysporum was found to be very effective in iron extraction and in the reduction of asbestos reactivity. We have used a combined proteomic approach to investigate changes in the fungal metabolic activities in the presence of crocidolite asbestos.

Abstract

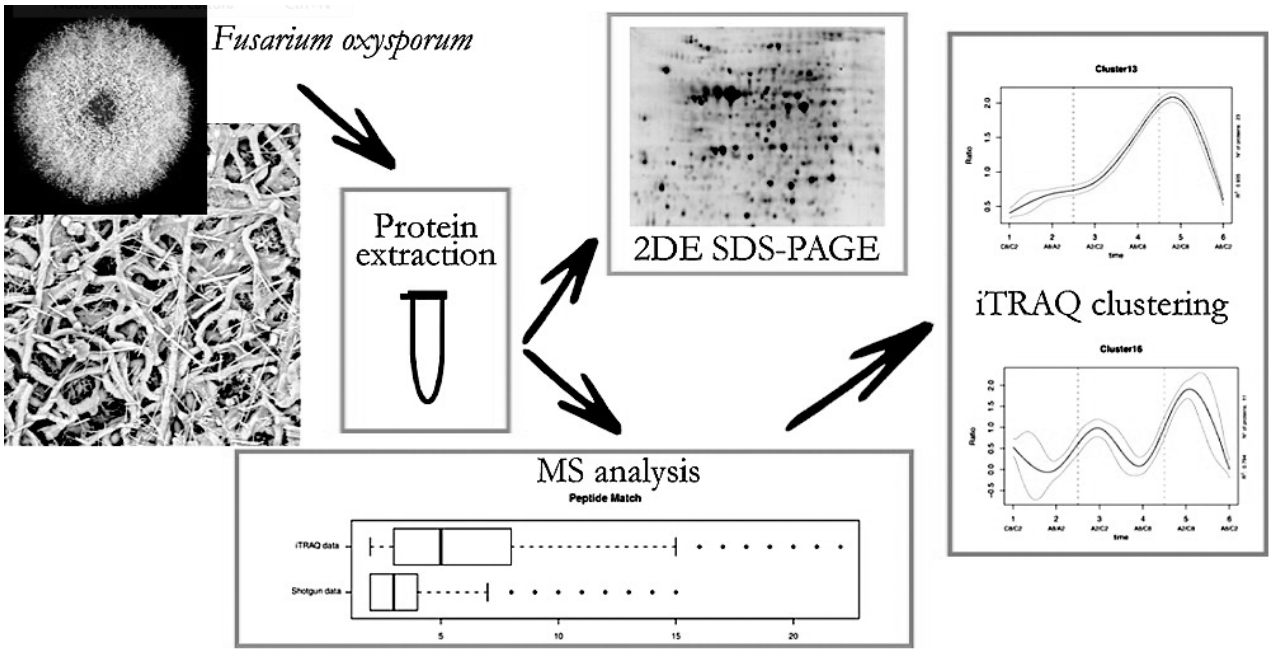

Cellular mechanisms of asbestos toxicity rely, at least in part, on the chemical composition of these minerals. Iron ions are directly involved in the accepted mechanism of fiber toxicity because they constitute active centers where release of free radicals and reactive oxygen species takes place. Although no current technology is available for the remediation of asbestos polluted sites, the soil fungus *Fusarium oxysporum* was found to be very effective in iron extraction from crocidolite asbestos *in vitro*, and to cause a significant reduction in asbestos surface reactivity and oxidative damage to naked DNA. As little information is available on the molecular mechanisms of the fungus−asbestos interactions, a combined proteomic approach that used 2-DE, shotgun and quantitative iTRAQ proteomics was used to investigate the fungal metabolic activities in the presence of crocidolite, an iron-rich type of asbestos. Although global proteomic analyses did not show significant changes in the protein expression pattern of *F. oxysporum* when exposed to asbestos fibers, some proteins specifically regulated by asbestos suggest up-regulation of metabolic pathways involved in protection from oxidative stress. When compared with the response to crocidolite observed by other authors in human lung epithelial cells, that unlike fungi

can internalize the asbestos fibres, a significant difference was the regulation of the pentose phosphate pathway.

Keywords:

Fusarium oxysporum; shotgun proteomics; iTRAQ; oxidative stress;asbestos

Introduction Asbestos is a generic commercial term given collectively to a group of fibrous hydrated silicate minerals that have been extensively mined and processed for industrial and commercial applications in the past centuries.(1) However, exposure to airborne asbestos fibrils can cause severe pneumoconiosis (asbestosis) and malignancies such as bronchogenic carcinoma and pleural mesothelioma,(2, 3) and both extraction and use of asbestos have been banned in many countries. Dismissed asbestos industries and mines have left substantial amounts of fibres on the previously occupied sites, and no current technology is available for the remediation of asbestos fibres dispersed over wide soil areas.

The mechanisms of asbestos toxicity in mammalian cells are not fully established but are thought to be multiple, including generation of reactive oxygen (ROS) and nitrogen (RNS) species, alteration in mitochondrial function, physical disturbance of cell cycle progression, and activation of several signal transduction pathways.(4) Some results also show that asbestos fibres, after phagocytosis by macrophages, might directly bind to proteins that regulate the cell cycle, the cytoskeleton, and the mitotic processes, contributing to significant spindle damage and chromosomal instability.(5)

Previous experiments have shown that a variety of soil fungi are able, at least *in vitro*, to grow in contact with asbestos and to extract iron from the fibers with variable effectiveness. *Fusarium oxysporum* was found to be very effective in iron extraction, likely through the release of chelating molecules.(6, 7) Crocidolite fibers pretreated with *F. oxysporum* showed a significant reduction in their surface reactivity (i.e., the ability of producing reactive hydroxyl radicals) and caused significantly less oxidative damage to naked DNA than control fibres.(8) Aim of the present work was to use a combined proteomic approach (2-DE, shotgun and quantitative iTRAQ) to investigate the alterations of the fungal biochemical activities caused by crocidolite asbestos. As fungal cells are surrounded by a rigid cell wall that prevents phagocytosis, this study may help to identify, in a eukaryotic system, those cellular effects of asbestos that are mediated by soluble factors.

Materials and Methods

Growth Conditions

F. oxysporum was grown in shaking conditions at 120 rpm in conical flasks at 25 °C in Czapek-glucose liquid medium [glucose 20 mg/mL, $NaNO_3$ 3 mg/mL, K_2HPO_4 1.31 mg/mL, $MgSO_4$ 0.5 mg/mL, $FeSO_4$ 0.01 mg/mL, KCl 0.5 mg/mL, MES (4-Morpholine ethane sulfonic acid) 3.9 mg/mL]. All reagents were purchased from Sigma. The dose of crocidolite fibres was expressed as weight/volume. The suspension of fibres added into the cultures after 14 days of growth (in the middle of the exponential phase) was thus prepared with 2.3 g of fibres in 100 mL of distilled water. Crocidolite was from UICC (Union Internationale Contre le Cancer) from the same batch employed

in previous research.(12) The control samples were mock inoculated with an equal volume of sterile distilled water. Fungal mycelia were collected by filtration after 1 h, 5 h, 1 day, 2 days, and 8 days, immediately frozen in liquid nitrogen, and stored at −80 °C before protein extraction.

Iron Release from Asbestos Fibers

Fe concentration in the culture medium after incubation with or without asbestos fibres was determined by inductively coupled plasma atomic emission spectrometry (ICP-AES) performed with a Liberty 100 Varian apparatus equipped with a V-Groove nebulizer and a Czerny-Turner monocromator (Department of Mineralogical and Petrological Science, University of Torino).

Protein Extraction

The mycelia of *F. oxysporum* were ground in liquid nitrogen and homogenized in cold extraction buffer [20 mM Na_2PO_4, pH 7.5, 2 mM PMSF (phenyl methyl sulphonyl fluoride), 1 mM EDTA (ethylenediaminetetracetic acid), and 8% PVPP (polyvinilpolypirrolidone)]. All reagents were purchased from Sigma. Crude homogenates were centrifuged at 4 °C (10 000g for 30 min). The supernatants were carefully removed, centrifuged again under the same conditions, and dialyzed overnight against Na_2PO_4 20 mM, EDTA 0.1 mM. Phenol saturated with 100 mM TrisHCl, pH 8 was added to the sample (1:1 v/v). After the sample was mixed for 30 min at 4 °C, the phenolic phase was separated by centrifugation. Proteins were precipitated overnight at −20 °C after adding 5 vol of 100% methanol containing 0.1 M ammonium acetate. The pellet recovered by centrifugation was rinsed with cold 100% methanol and 100% acetone and dried.

Two-Dimensional Gel Electrophoresis

Samples were resuspended in 650 μL of solubilization buffer containing 9 M urea and 2% Triton X-100. Protein content was determined by the method of Bradford, using bovine serum albumin (BSA) as a standard. Isoelectric focusing (IEF) was performed on immobilized pH gradient (IPG) strips in a Protean IEF Cell (Bio-Rad). Samples of 400 μg of proteins mixed with 2% (v/v) IPG buffer and 0.1 M dithiothreitol (DTT) were loaded on each IPG (Immobilized pH Gradient) strip and focused for 70 000 Vh at 15 °C after rehydration for 16 h. IPG strips were then either stored at −20 °C or immediately equilibrated for 10 min with each equilibration buffer (buffer 1, urea 6M; Tris-HCl 0.375 M, pH 8.8; glycerol 20%; SDS 2%; DTT 130 mM; buffer 2, urea 6M; Tris-HCl 0.375 M, pH 8.8; glycerol 20%; SDS 2%; iodoacetamide 35 mM). The 10% SDS-polyacrylamide homogeneous gels (0.1 cm ×19 cm ×23 cm) were polymerized overnight. Electrophoresis was run for 5 h at 10 °C under constant current (24 mA for each gel). Proteins separated on the polyacrylamide gel covered a molecular weight range of 9−200 kDa and p*I* of 4−7. Gels were fixed in 10% methanol and 7% acetic acid solution for 30 min and then stained with the SYPRO Ruby fluorescent dye (Molecular Probes) according to the manufacturer's instructions.

Shotgun Proteomics

The mycelial samples were extracted as described above. Two biological replicates were analyzed for each sample taken at 2 and 8 days, with 3 technical replicates each. Each sample was precipitated with ice-cold acetone overnight at −80 °C before being resuspended in 1 mL of 500 mM TEAB (triethylammonium bicarbonate) at pH 8.0. Samples were aliquoted in 0.1 mL fractions and proteins were reduced [50 mM TCEP (tris-(2-carboxyethyl) phosphine), incubated at 60 °C for 1 h], alkylated [200 mM MMTS (methylmethanethiosulfate), 10-min reaction time at room temperature], and digested with trypsin. Each sample was then vacuum-dried before being

resuspended in 10 mL of 0.1% TFA (Trifluoroacetic acid) for analysis with the Applied Biosystems QSTAR [ElectroSpray High performance quadrupole time-of-flight (ES-Qq-TOF)]. Aliquots of trypsin digests (typically 1−3 μL) were loaded onto an Ultimate nano-HPLC system (Dionex) equipped with a PepMap C18 trap (300 μm × 0.5 cm, Dionex) and an Onyx monolithic capillary column (100 μm × 15 cm, Phenomenex). The HPLC was interfaced with a QSTAR API Pulsar i Hybrid LC/MS/MS System (Applied Biosystems) with a MicroIonSpray source (fitted with 20 μm i.d. capillary). Positive ESI MS and MS/MS spectra were acquired over the range 350−1800 *m*/*z* using information dependent acquisition (IDA). Mass spectra were analyzed with the MASCOT software (http://www.matrixscience.com), using a local copy of the NCBInr released 20080608 database. The following modifications were permitted (mass change shown in daltons): carboxyamidomethylated cysteine (+57), oxidized methionine (+16), with MS/MS tolerance ±0.1 Da. Only proteins with *p*-value < 0.05 and identified by at least two peptides were considered.

iTRAQ Analysis

Control samples at times 2 and 8 days were labeled with iTRAQ reagents having molecular weights 114 and 115, respectively, whereas protein samples from mycelia exposed to crocidolite were labeled with iTRAQ reagents having molecular weights 116 and 117 Da, respectively. Samples were prepared according to the manufacturer's instructions using the iTRAQ Reagent (Applied Biosystems), which involves protein reduction and denaturation, blocking of the cysteines, protein digestion with trypsin, labeling of the digested proteins, and pooling of the labeled digests. The labeled peptide mixture was separated by sample fractionation using offline strong cation exchange (SCX) chromatography to lower the complexity of the mixture.(9)

This step prior to LC-MS/MS has been employed in several studies of whole-cell lysates.(10, 11)The column (PolyCationLC 200 mm 2 mL loop) was equilibrated with buffer A (10 mM KH_2PO_4, 25% ACN, H_3PO_4 to adjust the pH < 3) and eluted with a linear gradient of buffer B (10 mM KH_2PO_4, 25% ACN, 1 M KCl, H_3PO_4 to adjust the pH < 3). Four gradient steps were used: from 0% to 15% solvent B, followed by 15−50%, 50−80% solvent B. On the basis of the UV (214 nm) trace, 62 fractions were selected for further separation by reverse phase HPLC (RP-HPLC),(22)and were completely dried and stored at −20 °C.

Each protein fraction was separated by RP-HPLC (Dionex UltiMate NanoHPLC) in two steps: 18 min gradient from 1% to 50% solvent B [100% acetonitrile (ACN), 0.1% Heptafluorobutyric Acid (HFBA)] and 1 min gradient from 50% to 85% solvent B. Solvent A was 2% ACN and 0.1% HFBA in water. The eluent from RP-HPLC separation was mixed with a solution of 5 mg/mL matrix (α-cyano-4-hydrocinnamic acid) in 75% ACN, 0.1% TFA (trifluoroacetic acid) and 15 mg/mL ammonium citrate. The sample combined with the matrix was continuously delivered from the syringe pump of the Probot system and spotted on a stainless steel MALDI plate every 6 s during the peptides' eluting phase. Six mass calibration standards were manually spotted on the plate. MS and MS/MS analyses were performed on a 4700 Proteomics Analyzer matrix-assisted laser desorption ionization (MALDI) time-of-flight (TOF) mass spectrometer. After plate alignment and calibration, an MS spectrum was acquired from all spots on each plate.

MS Data Analysis

Positive-ion MALDI mass spectra were obtained using an Applied Biosystems 4700 Proteomics Analyzer (Applied Biosystems, Foster City, CA) in reflectron mode. MS spectra were acquired over a mass range of *m*/*z* 800−4000. Monoisotopic masses were obtained from centroids of raw,

unsmoothed data. The 10 strongest peaks, with a signal-to-noise greater than 50, from each fraction were selected for CID-MS/MS analysis. A fraction-to-fraction precursor exclusion of 200 ppm was used. For CID-MS/MS, a Source 1 collision energy of 1 kV was used, with air as the collision gas. The precursor mass window was set to a relative resolution of 50, and the metastable suppressor was enabled. The default calibration was used for MS/MS spectra, which were baseline-subtracted (peak width 50) and smoothed (Savitsky-Golay with three points across a peak and polynomial order 4); peak detection used a minimum S/N of 5, local noise window of 50 *m*/*z*, and minimum peak width of 2.9 bins. Mass spectral data obtained in batch mode were submitted to database searching using TS2Mascot (Matrix Science, version 1.0.0). A locally running copy of the Mascot program (Matrix Science Ltd., version 2.1) was used to perform the searches using the NCBInr protein database. We used as fixed modifications: iTRAQ4plex (K), Methylthio (C), iTRAQ4plex (N-term), iTRAQ4plex (K); as variable modifications, Oxidation (M). A minimum confidence of 95% ($P < 0.05$) was used for peptide identification as defined by the GPS software. Trypsin was specified as the proteolytic enzyme and one miss cleavage was allowed. Mass tolerance was set at 200 ppm for peptide precursors and at 0.1 Da for fragment ions. We used MudPIT scoring and as peptide threshold “at least homology”. Only proteins with *p*-value < 0.05 and identified by at least two peptides were considered. All quantitative results were calculated based on default bias-corrections applied.

Results and Discussion

F. oxysporum is a fungus ubiquitously distributed in many soil types, and previous experiments showed that growth of this fungus was not significantly affected by crocidolite asbestos.(12)Consistent with these previous observations, growth of *F. oxysporum* was not affected by asbestos in the current experiment (data not shown).

Crocidolite fibres were added as aqueous suspension in the middle of the exponential fungal growth, and mycelia exposed to asbestos fibers, as well as mock inoculated mycelia, were harvested after 1 h, 5 h, 1 day, 2 days, and 8 days to investigate short-term responses of *F. oxysporum* to asbestos exposure. Mycelial samples were frozen immediately in liquid nitrogen and stored at −80 °C. Proteins were extracted from the fungal mycelia and processed either for 2-DE separation or gel-free analyses.

2-DE Analysis Indicates an Early Response of *F. oxysporum* to Crocidolite

Figure 1 summarizes the results of 2-DE separation. Figure 1A shows the protein profiles of *F. oxysporum* at the different time-points. For each experimental condition, 3 biological replicates were analyzed, with 3 technical replicates each. Molecular weight of proteins separated on the 2-DE polyacrylamide gels ranged from 9 to 200 KDa and p*I* from 4 to 7.

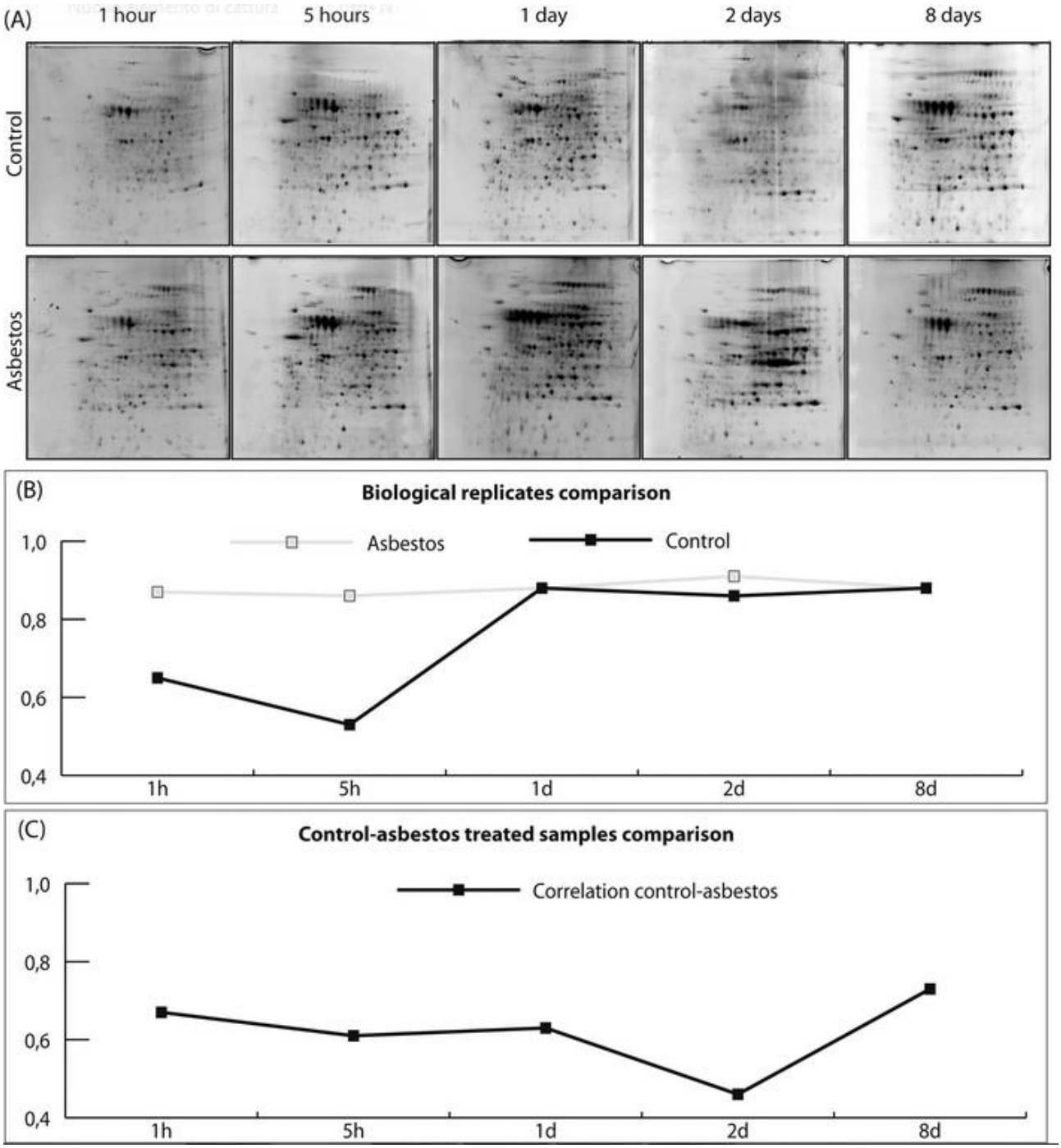

Figure 1. 2-DE separation of *F. oxysporum* proteins expressed during a time-course experiment in the presence and absence of crocidolite asbestos (for each time-point, we performed 3 biological replicates). One representative gel for each time-point is shown (A). Correlation coefficients of the biological replicates of both control and asbestos treated samples, as calculated by the PDQuest program (B). Correlation coefficients of the biological replicates of control samples and asbestos treated samples at each individual time-point, as calculated by the PDQuest program (C).

For each time-point, the correlation coefficient (CC) among protein profiles obtained after 2-DE separation was calculated with the PDQuest software (version 7.1) (Bio-Rad) for both technical and biological replicates. CC values above 0.8 were found for all technical replicates, indicating

good reproducibility of protein separation. For the biological replicates (Figure 1B), a CC above 0.8 was obtained for all asbestos treated samples, whereas it varied for the control samples. CC was very low for mock inoculated control samples after 1 and 5 h, but it raised above 0.8 for the last three time-points (1, 2, and 8 days). Finally, we compared the 2-DE profiles obtained for control and asbestos treated samples at each time-point (Figure 1C). For the last three time points, showing good reproducibility, the CC reached the lowest value 2 days after crocidolite addition, but it raised after 8 days to reach the highest value (Figure 1C). The time-course experiment thus indicates that protein expression by *F. oxysporum* was significantly affected after a short-term exposure to crocidolite asbestos (2 days), but it also suggests that metabolic activities returned similar to the control mycelium relatively quickly (8 days). These two experimental time-points were chosen for further analyses by shotgun and iTRAQ proteomic methods because they showed differential protein expression as well as good reproducibility.

Global Analysis of Shotgun and iTRAQ Proteomic Data

After mass spectrometry, we identified a total of 328 proteins with shotgun (p-value < 0.05 and at least two peptides) and 554 proteins with iTRAQ (p-value < 0.05 and at least two peptides). On average, we found a protein match of 3.2 peptides per protein with the shotgun analysis, and 5 peptides per protein with the iTRAQ labels (Figure 2). In general, there was good agreement between the statistical results (peptide match, peptide length, and protein cover) obtained in this study and data from the literature.(13-15)

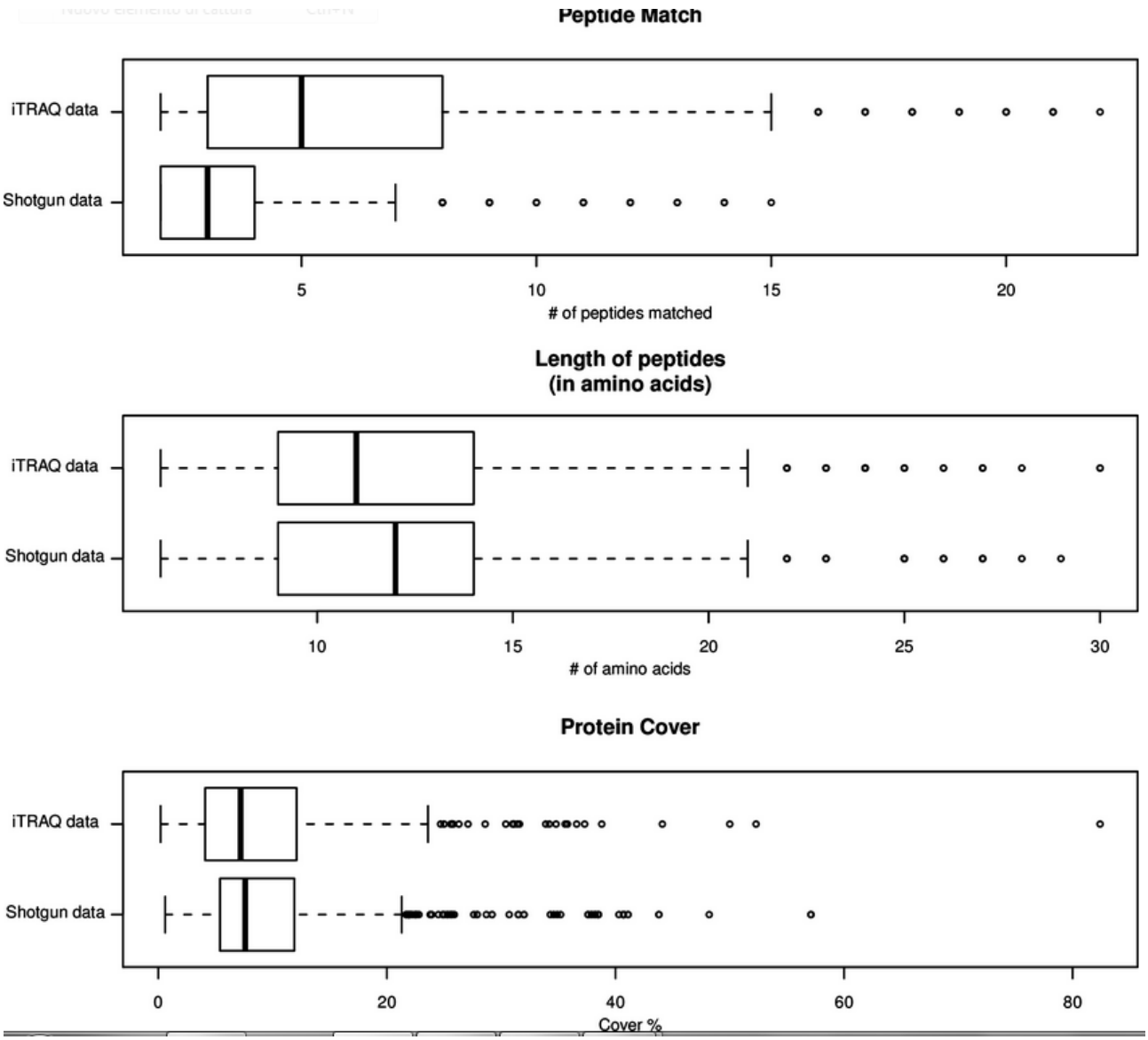

Figure 2. Graphic summaries of iTRAQ and shotgun proteomic data. Boxplots represent peptide match, length of peptides, and protein cover. The middle line in each box is the median data value, and the left and right box extremes are the 25th and 75th percentiles, respectively. The boxplot 'whiskers' extend to extreme data values not considered outliers, and open circles indicate potential outlying values.

The complete list of proteins identified by shotgun proteomics and their occurrence in the different samples is provided in Table 1S (Supporting Information), and the corresponding Venn diagram is shown in Figure 3. After 2 days, we could identify in total 126 proteins in the control samples (referred to as "C2d") and 148 proteins in the asbestos treated samples (referred to as "A2d"). After 8 days, 214 proteins were identified in the control samples (referred to as "C8d") and 192 in the asbestos treated samples (referred to as "A8d"). The largest group in the Venn diagram (67 identified proteins) comprised proteins in common between all samples, including cytoskeletal components, molecular chaperones, and many enzymes involved in carbohydrate metabolism (Table 1S, Supporting Information). Analysis of the data using functional annotations with the

KAAS (KEGG Automatic Annotation Server)(16, 17) and the BLAST2GO(18) tools at the two time-points did not reveal significant alterations in *F. oxysporum* caused by crocidolite (data not shown).

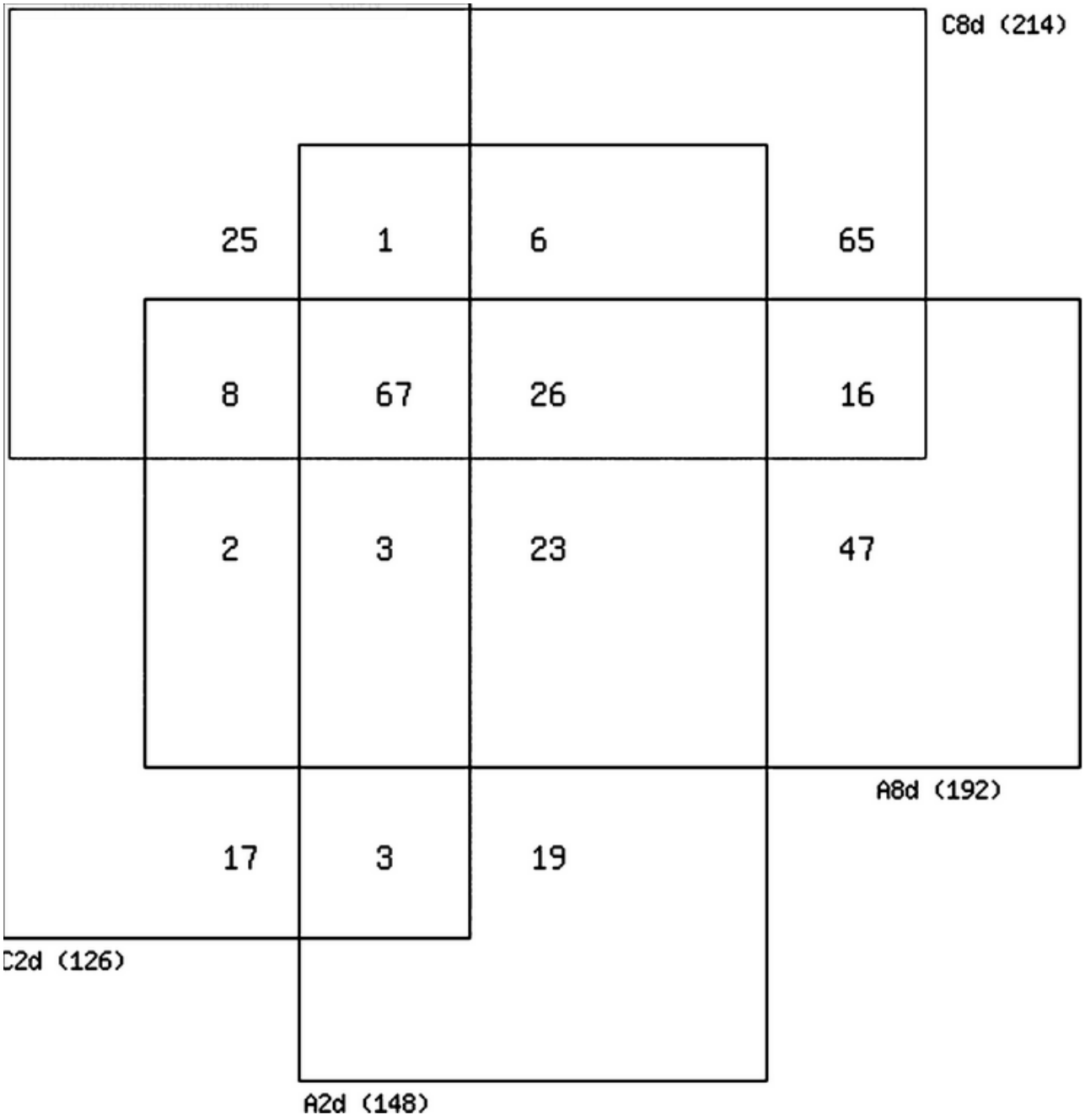

Figure 3. Venn diagram reporting the number of proteins identified in the shotgun experiment by mass spectrometry that were either unique to specific treatments or shared among the different conditions tested: control samples after 2 days (C2d) and after 8 days (C8d), asbestos treated samples after 2 days (A2d) and 8 days (A8d). Total protein numbers for each sample are also shown.

Most proteins sharing the same function were identified by shotgun proteomics in all *F. oxysporum* samples, although a regulation in their expression/accumulation, caused by asbestos, could not be excluded. Shotgun proteomics is not a quantitative method, even though the number of protein isoforms (as identified by the number of different peptides) may mirror protein abundance.(19, 20) We have, therefore, used multiplex isobaric labeling with iTRAQ reagents to quantify protein expression/accumulation in *F. oxysporum* exposed to crocidolite fibers relative to the control samples. The iTRAQ data were analyzed by Smoothing Spine Clustering (SSC) in order to visualize quantitative protein variations in *F. oxysporum* during the time course experiment and in the different experimental conditions.

Smoothing Spline Clustering (SSC) is a statistical method for clustering time-series gene expression data and was used here for the first time with iTRAQ data to group proteins with similar expression patterns in the different treatments. A distinguishing feature of SSC is that it accurately estimates individual gene expression profiles and the mean gene expression profile within clusters simultaneously, making it extremely powerful for clustering time course data.(21)

Starting with an initial cluster of $k = 4$ based on k-means clustering, the 554 proteins were grouped by SSC into a final set of 18 clusters (shown in Figures 4 and 1S, Supporting Information), according to their profiles. The list of proteins identified in each cluster, together with their relative abundance, is provided in Table 2S in Supporting Information. On the basis of previous proteomic studies,(22, 23) proteins were considered as not being regulated by the presence of asbestos when the iTRAQ labeled ratio ranged from 0.8 to 1.2.

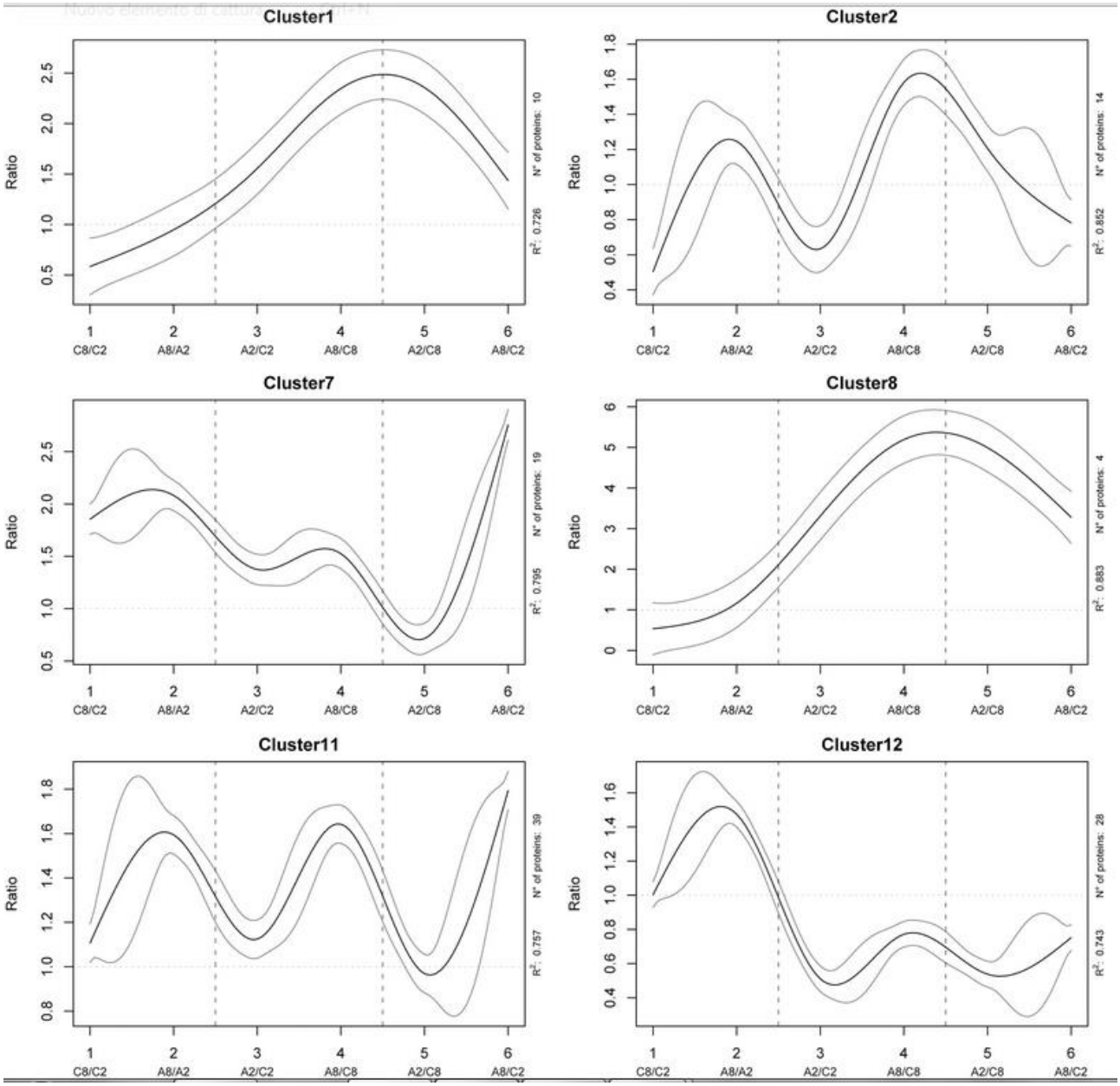

Figure 4. Clustering of iTRAQ expression data by Smoothing Spine Clustering. Estimated mean expression curves (solid lines) and 95% confidence bands (gray bands) for six representative clusters out of the 18 discovered by SSC in the *F. oxysporum* iTRAQ data. Protein quantity is expressed as a ratio between two experimental conditions. Points 1 and 2 indicate changes in expression over time in the same treatment (control or asbestos treated mycelia), points 3 and 4 indicate regulation of protein expression depending on the treatment, whereas points 5 and 6 represent disassorted pairings. The remaining clusters are shown in Figure 1S, Supporting Information.

Some of the clusters in Figures 4 and 1S in Supporting Information (1, 7, 8 and 9) showed, at both time points, a significant up-regulation of proteins in the *F. oxysporum* mycelium exposed to asbestos as compared to the corresponding control samples. Proteins in clusters 11 and 13 (Figures 4 and 1S in Supporting Information) were up-regulated in the asbestos-treated samples, but the values were significant only after 8 days of exposure. By contrast, cluster 12 (Figure 4) grouped proteins that were down-regulated by asbestos at both time points. The other clusters showed mixed expression patterns of down- and up-regulation over the time course. Apart from some exceptions, like proteins in clusters 8 and 10, variations in protein expression levels were usually modest.

Accumulation of Specific *F. oxysporum* Proteins Is Regulated by Crocidolite

Two strongly up-regulated proteins in clusters 1 and 8 (up to 2.8- and 4.9-fold 8 days after exposure to crocidolite, respectively) were homologous to the rapamycin binding FKBP proteins (Table 2S, Supporting Information). Together with cyclophilins, FKBP proteins belong to immunophilins and show peptidyl prolyl *cis*/*trans* isomerase (PPIase) activity. Studies in both animal and plant systems have revealed a diverse array of functions for individual immunophilin members.(24, 25) Such functions can be a result of their protein foldase activity, chaperone activity, scaffolding activity, and other unknown activities. A very clear distinction between immunophilins and other types of protein foldases and molecular chaperones is that each member of the immunophilin family appears to have specific targets and function in the cell. FKBP12 in particular can be a physiological regulator of the cell cycle, as it modulates signal transduction events required for G1 to S phase cell cycle progression in yeast and mammalian cells.(26, 27) Although the functions of the FKBP12 proteins in *F. oxysporum* is not known, it was interesting to note that different histone isoforms were down-regulated by asbestos (cluster 12, Table 2S). These data may suggest that, although there was not a significant change in fungal growth in the presence of crocidolite, DNA synthesis and cell division were nevertheless reduced.

Two cyclophilins were identified as being up-regulated by crocidolite (up to 2.6-fold after 8 days) in clusters 10 and 11 (Table 2S). By contrast, other molecular chaperones were generally expressed constitutively in all samples, with the exception of the 90 kDa heat shock protein in cluster 11 (Table 2S). This suggests a specific induction of immunophilins by crocidolite, rather than a generalized stress response.

The plasma membrane proton pump-ATPase in cluster 10 (Table 2S and Figure 1S, Supporting Information) was one of the proteins more strongly up-regulated by crocidolite (4.7-fold after 8 days of exposure). As a primary transporter, proton pump-ATPase (H^+-ATPase) mediates ATP-dependent proton extrusion to the extracellular space, thus, creating pH and potential differences across the plasma membrane that activate a large set of secondary transporters. The H^+-ATPase therefore plays a central role in transport across the plasma membrane. The role of H^+-ATPase in the *F. oxysporum* response to crocidolite is unclear. In some plants, acidification of the rhizosphere by the plasma membrane H^+-ATPase helps to mobilize sparingly soluble Fe that is otherwise not available to the plant, and Fe deficiency induces responses that involve modulation of an H^+-ATPase gene at the transcriptional level.(28) However, in our experiment, *F. oxysporum* very unlikely experienced iron deficiency. Iron was supplemented to the medium and, together with the iron released by fungal activity from the crocidolite fibers, reached a concentration of 16.90 (±1.34) ppm after 2 days and 23.58 (±1.74) ppm after 8 days, according to the analysis performed by ICP-AES. Both values were significantly higher if compared with the mock inoculated samples, respectively, 0.95 (±0.17) ppm and 1.09 (± 0.17) ppm for the two sampling times. Other roles must

be therefore envisaged for this strongly up-regulated membrane protein. In soybean, up-regulation of plasma membrane H^+-ATPase activity was induced by metal cations such as aluminum at both transcriptional and translational level.(29) In this plant, up-regulation of H^+-ATPase was associated with an increased secretion of citrate from roots, a natural metal chelator that binds to metal cations and protects plant cells from metal toxicity. Although increased secretion of organic acids has been observed in filamentous fungi in response to heavy metals,(7, 30) a correlation with H^+-ATPase has not been described.

Specific Protein Markers Suggest That Crocidolite Induces Oxidative Stress in *F. oxysporum*

One way crocidolite fibres affect animal cells is through the release of iron ions. Asbestos in fact catalyzes many of the same reactions that iron does, including lipid peroxidation and DNA damage.(31) Iron in the fiber matrix or complexed at the surface has been demonstrated to participate in the catalysis of reactive oxygen species.(32, 33) Reactive oxygen species (ROS) such as superoxide and hydrogen peroxide are byproducts of normal aerobic metabolism, produced mainly by partial reduction of oxygen during respiration. The highly reactive hydroxyl radicals are then generated by the presence of hydrogen peroxide and iron (Fenton reaction). Hydroxyl radicals can oxidize virtually any cell molecule, causing DNA damage, protein inactivation, protein cross-linking and fragmentation, and lipid peroxidation.(34) *F. oxysporum* is capable of actively releasing significant amounts of iron from crocidolite asbestos fibres (this study,(7, 12)), thus, increasing the metal concentration in the medium and in the mycelium. As a consequence, lipid peroxidation can occur in the *F. oxysporum* mycelium exposed to crocidolite, with an increase in malondialdehyde (MDA; Daghino, S., unpublished results).

Identification of some specific proteins by both shotgun and iTRAQ proteomics suggests that the mycelium is experiencing an oxidative stress, likely due to the increased concentration of iron in the culture medium and in the mycelium following solubilization from the crocidolite fibers.

A protein specifically associated with the two asbestos treated samples (A2 + A8d in Table 1S, Supporting Information) in the shotgun experiment was a thiol-specific antioxidant (TSA) protein homologous to TSA1 of *Ajellomyces capsulatus*. This protein groups with the peroxiredoxins, also called thioredoxin peroxidases, and belongs, together with glutathione peroxidases, to the larger class of thiol-dependent peroxidases. Their distribution in the genome of yeast and filamentous fungi has been recently investigated.(35) As shown by Netto et al.,(36) the antioxidant property of TSA is due at least in part to its ability to remove H_2O_2, thereby preventing the formation of reactive species during the iron-catalyzed oxidation of thiol compounds. High concentrations of either mercaptoethanol, iron, or O_2 induced the synthesis of TSA.(36) In addition to this specific protein, other peroxiredoxins, identified by different peptides in the shotgun experiment, were found to be expressed by *F. oxysporum* both in asbestos treated and control samples (Table 1S, Supporting Information). TSA was not identified in the iTRAQ experiment, but a periredoxin was found to be up-regulated by asbestos in Clusters 18 (Table 2S, Supporting Information).

Other protein markers that suggest a response to oxidative stress in *F. oxysporum* exposed to crocidolite are the bifunctional catalase-peroxidases. Catalase-peroxidases in pro- and eukaryotic cells are important enzymes to cope with reactive oxygen species, as they are good scavengers for hydrogen peroxide.(37) They were identified by shotgun proteomics in the A8d sample (Table 1S) and found by iTRAQ to be up-regulated in the asbestos treated samples after 8 days of exposure (clusters 9, 11, 17 in Table 2S).

Some peptides specifically found by shotgun proteomics in the asbestos treated *F. oxysporum*samples matched two proteins (Table 1S, Supporting Information) that correspond to enzymes involved in thiamine biosynthesis. Thiamine (vitamin B1) is an essential vitamin that acts as a key cofactor of enzymes involved in basic processes of carbohydrate metabolism such as glycolysis, the citric acid cycle, and the pentose-phosphate cycle. Recently, thiamine has been also found to confer enhanced tolerance to oxidative stress in *Arabidopsis*.(38) Thiamine biosynthesis occurs through a multistep pathway, involving two independent branches that synthesize the thiazole and pyrimidine moieties of thiamine, respectively.(39) A thiamine biosynthetic enzyme homologous to the NMT1 (*N*-myristoyltransferase 1) protein of *Aspergillus clavatus* was found in the asbestos treated samples at both time points, whereas a protein corresponding to the stress-inducible thiazole biosynthetic enzyme sti35 of *F. oxysporum* was found only 2 days after exposure to crocidolite. Proteins involved in thiamine biosynthesis were identified in *F. oxysporum* also by iTRAQ. A protein homologue of NMT1 protein of *Fusarium graminearum* and a protein homologue of the thiamine biosynthesis protein of *Coccidioides immitis* (cluster 2 in Table 2S) were both up-regulated (2-fold) by asbestos after 8 days of exposure. The protein homologue of the thiazole biosynthetic enzyme sti35 of *F. oxysporum*was also identified by iTRAQ, but showed constitutive expression.

Antioxidant Response of *F. oxysporum* through Metabolic Rerouting

In addition to specific compounds, eukaryotic cells can counteract the deleterious consequences of oxidative stress by metabolic alterations involving the glycolytic pathway. Glyceraldehyde 3-phosphate dehydrogenase (GAPDH) catalyzes a crucial step of glycolysis, but recent evidence implicates GAPDH in other cellular processes. For example, GAPDH acts as a reversible metabolic switch under oxidative stress.(40) When cells are exposed to oxidants, they need excessive amounts of the antioxidant cofactor NADPH, which is synthesized in the cytosol through the pentose phosphate pathway. Oxidant-treatments cause inactivation of GAPDH, as well as of other enzymes in the glycolytic pathway. This inactivation reroutes temporally the metabolic flux from glycolysis to the pentose phosphate pathway, allowing the cell to generate more NADPH.(40)

In the iTRAQ experiment, GAPDH was highly represented in cluster 12 (Figure 4, Table 2S), grouping proteins down-regulated by asbestos at both experimental time points and in cluster 2 (Figure 1S, Table 2S), grouping proteins that were not detected in the A2d samples. In particular, most GAPDH proteins in Cluster 12 were more strongly down-regulated 2 days after addition of the crocidolite fibres, with a slight increase in protein amounts after 8 days.

Other enzymes involved in the glycolytic pathway were also found to be down-regulated after 2 days of exposure to asbestos fibers, like glucose-6-phosphate isomerase (cluster 13), some of the triose phosphate isomerase isoforms (clusters 4 and 13), enolase (clusters 13 and 17), and pyruvate kinase (clusters 12 and 5). All these enzymes increased significantly above the controls after 8 days of exposure to crocidolite.

Consistently with the down-regulation of GAPDH in *F. oxysporum*, there was a significant up-regulation of key enzymes involved in the pentose phosphate pathway. In particular, up-regulated proteins (up to 2.3-fold) in cluster 7 and 10 (Table 2S) corresponded to 6-phosphogluconate dehydrogenase, which catalizes the first NADPH-producing reaction in the pentose phosphate pathway. Proteins corresponding to 6-phosphogluconate dehydrogenase were also specifically identified by shotgun proteomics in the two asbestos treated samples (Table 1S). Hexokinase, an enzyme found in cluster 7 (Figure 1S and Table 2S), phosphorylates glucose to glucose-6-

phosphate and prepares it for later steps either in the glycolytic or in the pentose phosphate pathway. Its up-regulation (1.5-fold) 2 days after exposure to crocidolite, together with up-regulation of other enzymes in the pentose phosphate pathway, suggests that the synthesis of glucose-6-phosphate is sustained to feed it into this pathway. Although protein abundance does not necessarily reflect catalytic activity, down-regulation of enzymes involved in the glycolytic pathway and up-regulation of enzymes involved in the pentose phosphate pathway in the A2d sample suggest that metabolic rerouting may be an important early mechanism of oxidant resistance in *F. oxysporum*.

The mitochondrion is a vulnerable intracellular target to reactive oxygen species (ROS), and the expression of ATP synthase, the enzyme responsible for the mitochondrial production of ATP from ADP, has been used to monitor mitochondrial damage.(41) These authors found that oxidative injury of pancreatic cells resulted in the induction of mitochondrial ATP synthase. Subunits of the mitochondrial ATP synthase complex in *F. oxysporum* were consistently grouped in clusters 7 and 11 (Figure 1S and Table 2S) and sporadically found in other clusters. These proteins were up-regulated in response to exposure to crocidolite (up to 2.6-fold), and may represent another marker indicating oxidative stress in *F. oxysporum* exposed to crocidolite.

Concluding Remarks

In conclusion, a combined proteomic approach allowed us to investigate the cellular responses of the filamentous fungus *F. oxysporum* to crocidolite asbestos. The results of shotgun and iTRAQ proteomics were generally consistent and complementary, apart from a few cases. For example, the shotgun experiment revealed a striking difference between asbestos treated and control mycelia in the number of peptides matching translation elongation factors, suggesting that crocidolite strongly down-regulates the accumulation of both elongation factor 1 alpha and factor 2, especially after short exposure to the fibres (2 days). Unfortunately, most peptides matching translation elongation factors (cluster 15) could not be quantitated after iTRAQ labeling due to the low confidence in protein identification probability. For those proteins that could be quantified (cluster 14), no changes in protein accumulation were observed in the different samples.

Taken together, our results suggest that *F. oxysporum*'s ability to release iron from asbestos fibers(7, 12) results in increased oxidative stress. Mechanisms of defense against this increased oxidative stress seem to involve enzymes such as periredoxins and bifunctional catalase-peroxidases, two hydrogen peroxide-detoxifying enzymes, as well as antioxidant metabolites such as thiamine. By contrast, we could not detect enzymes involved in glutathione biosynthesis, although glutathione peroxidase, another scavenger of hydrogen peroxide that oxidizes monomeric glutathione, was slightly up-regulated in the A2d sample.

As an early response to asbestos, *F. oxysporum* also seems to reroute the carbohydrate flux from glycolysis to the pentose phosphate pathway to counteract perturbations in the cytoplasmic redox state. The NADPH generated in the pentose phosphate pathway plays a central role in cellular ROS metabolism, as it is the reducing equivalent for many detoxifying pathways. Catalase, an enzyme induced by asbestos in *F. oxysporum*, depends on NADPH, as this molecule protects the protein from being inactivated by the substrate.(42)

The metabolic rerouting observed in *F. oxysporum* in response to crocidolite is in striking contrast with the behavior of mammalian cells exposed to the same asbestos fibers.(43) In human lung epithelial cells, crocidolite fibers caused a dose- and time-dependent inhibition of the pentose

phosphate pathway through the inhibition of the glucose-6-phosphate dehydrogenase, a key enzyme of this pathway. Experiments in a cell-free system suggest that crocidolite inhibits the enzyme by directly interacting with the protein,(43) a situation that may occur *in vivo* when the fibers are internalized by the cell and can enter into close contact with this cytosolic enzyme. As fungi are surrounded by a rigid cell wall, internalization of the asbestos fiber is prevented in *F. oxysporum*, and the absence of direct contact with the cell components may explain the different metabolic responses. Thus, the results obtained in *F. oxysporum* may also help to understand, when compared with other biological systems, the cellular mechanisms of asbestos toxicity that are independent from fiber phagocytosis.

Acknowledgment

We thank Jerry Thomas, Adam Dowle and David Ashford (University of York, U.K.) for assistance in mass spectrometry and shotgun proteomics analyses. Research was partly funded by Regione Piemonte, by the Fondazione SanPaolo and by the University of Torino.

Supporting Information

A complete list of proteins identified by MASCOT in the four *F. oxysporum* samples after the shotgun proteomics experiment, as well as the list of proteins quantified by iTRAQ and clustered according to their ratio in the different samples, are provided. This material is available free of charge via the Internet at http://pubs.acs.org.

References

1. Lee, R. J.; Strohmeier, B. R.; Bunker, K. L.; Van Orden, D. R. Naturally occurring asbestos: a recurring public policy challenge *J. Hazard. Mater.* 2008, 153, 1– 21
2. Mossman, B. T.; Churg, A. Mechanisms in the pathogenesis of asbestosis and silicosis*Am. J. Resp. Crit. Care* 1998, 157, 1666– 1680
3. Shukla, A.; Ramos-Nino, M.; Mossman, B. Cell signaling and transcription factor activation by asbestos in lung injury and disease *Int. J. Biochem. Cell Biol.* 2003, 35, 1198–1209
4. Upadhyay, D.; Kamp, D. W. Asbestos-induced pulmonary toxicity: role of DNA damage and apoptosis *Exp. Biol. Med.* 2003, 228, 650– 659
5. Ault, J .G.; Cole, R. W.; Jensen, C. G.; Jensen, L. C.; Bachert, L. A.; Rieder, C. L. Behavior of crocidolite asbestos during mitosis in living vertebrate lung epithelial cells *Cancer Res.*1995, 55, 792– 798
6. Martino, E.; Cerminara, S.; Prandi, L.; Fubini, B.; Perotto, S. Physical and biochemical interactions of soil fungi with asbestos fibers *Environ. Toxicol. Chem.* 2004, 23, 938–944
7. Martino, E.; Prandi, L.; Fenoglio, I.; Bonfante, P.; Perotto, S.; Fubini, B. Soil fungal hyphae bind and attack asbestos fibers *Angew. Chem., Int. Ed.* 2003, 42, 219– 222
8. Daghino, S.; Turci, F.; Tomatis, M.; Favier, A.; Perotto, S.; Douki, T.; Fubini, B. Soil fungi reduce the iron content and the DNA damaging effects of asbestos fibers *Environ. Sci. Technol.* 2006, 40, 5793– 5798

9. Evans, F. F.; Raftery, M. J.; Egan, S.; Kjelleberg, S. Profiling the secretome of the marine bacterium *Pseudoalteromonas tunicata* using amine-specific isobaric tagging (iTRAQ) *J. Proteome Res.* 2007, 6, 967– 975
10. Aggarwal, K. C.; Leila, H.; Lee, K. H. Quantitative analysis of protein expression using amine-specific isobaric tags in Escherichia coli cells expressing rhsA elements *Proteomics*2005, 5, 2297– 2308
11. Wolff, S.; Otto, A.; Albrecht, D.; Zeng, J. S.; Büttner, K.; Glückmann, M.; Hecker, M.; Becher, D. Gel-free and gel-based proteomics in Bacillus subtilis: a comparative study *Mol. Cell. Proteomics* 2006, 5, 1183– 1192
12. Daghino, S.; Martino, M; Fenoglio, I.; Tomatis, M.; Perotto, S.; Fubini, B. Inorganic materials and living organisms: surface modifications and fungal responses to various asbestos forms *Chemistry* 2005, 11, 5611– 5618
13. Dowell, J. A.; Frost, D. C.; Zhang, J.; Li, L. Comparison of two-dimensional fractionation techniques for shotgun proteomics *Anal. Chem.* 2008, 80, 6715– 6723
14. Ross, P. L.; Huang, Y. L. N.; Marchese, J. N.; Williamson, B.; Parker, K.; Hattan, S.; Khainovski, N.; Pillai, S.; Dey, S.; Daniels, S.; Purkayastha, S.; Juhasz, P.; Martin, S.; Bartlet-Jones, M.; He, F.; Jacobson, A.; Pappin, D. J. Multiplexed protein quantitation in*Saccharomyces cerevisiae* using amine-reactive isobaric tagging reagents *Mol. Cell. Proteomics* 2004, 3, 1154– 1169
15. Zhen, Y.; Xu, N.; Richardson, B.; Becklin, R.; Savage, J. R.; Blake, K.; Peltier, J. M.Development of an LC-MALDI method for the analysis of protein complexes *J. Am. Soc. Mass Spectrom.* 2004, 15, 803– 822
16. Kanehisa, M.; Goto, S.; Furumichi, M.; Tanabe, M.; Hirakawa, M. KEGG for representation and analysis of molecular networks involving diseases and drugs *Nucleic Acids Res.* 2010,38, D355– 360
17. Kanehisa, M.; Goto, S.; Hattori, M.; Aoki-Kinoshita, K. F.; Itoh, M.; Kawashima, S.; Katayama, T.; Araki, M.; Hirakawa, M. From genomics to chemical genomics: new developments in KEGG *Nucleic Acids Res.* 2006, 34, D354– 357
18. Götz, S.; García-Gómez, J.; Terol, J.; Williams, T.; Nagaraj, S.; Nueda, M.; Robles, M.; Talón, M.; Dopazo, J.; Conesa, A. High-throughput functional annotation and data mining with the Blast2GO suite *Nucleic Acids Res.* 2008, 36, 3420– 3435
19. Rappsilber, J.; Ryder, U.; Lamond, A. I.; Mann, M. Large-scale proteomic analysis of the human splicesome *Genome Res.* 2002, 12, 1231– 1245
20. Sanders, S. L.; Jennings, J.; Canutescu, A.; Link, A. J.; Weil, P. A. Proteomics of the eukaryotic transcription machinery: identification of proteins associated with components of yeast TFIID by multidimensional mass spectrometry *Mol. Cell. Biol.* 2002, 22, 4723–4738
21. Ma, P.; Castillo-Davis, C. I.; Zhong, W.; Liu, J. S. A data-driven clustering method for time course gene expression data *Nucleic Acids Res.* 2006, 34, 1261– 1269
22. Hill, E. G.; Schwacke, J. H.; Comte-Walters, S.; Slate, E. H.; Oberg, A. L.; Eckel-Passow, J. E.; Therneau, T. M.; Schey, K. L. A statistical model for iTRAQ data analysis *J. Proteome Res.* 2008, 7, 3091– 3101
23. Xu, J.; Khor, K. A.; Sui, J.; Zhang, J.; Tan, T. L.; Chen, W. N. Comparative proteomics profile of osteoblasts cultured on dissimilar hydroxyapatite biomaterials: an iTRAQ-coupled 2-D LC-MS/MS analysis *Proteomics.* 2008, 8, 4249– 4258
24. Göthel, S. F.; Marahiel, M. A. Peptidyl-prolyl cis-trans isomerases, a superfamily of ubiquitous folding catalysts *Cell. Mol. Life Sci.* 1999, 55, 423– 436

25. He, Z.; Li, L.; Luan, S. Immunophilins and parvulins. Superfamily of peptidyl prolyl isomerases in *Arabidopsis Plant Physiol.* 2004, 134, 1248– 1267
26. Aghdasi, B.; Ye, K.; Resnick, A.; Huang, A.; Ha, H. C.; Guo, X.; Dawson, T. M.; Dawson, V. L.; Snyder, S. H. FKBP12, the 12-kDa FK506-binding protein, is a physiologic regulator of the cell cycle *Proc. Natl. Acad. Sci. U.S.A.* 2001, 98, 2425– 2430
27. Cardenas, M. E.; Heitman, J. FKBP12-rapamycin target TOR2 is a vacuolar protein with an associated phosphatidylinositol-4 kinase activity *EMBO J.* 1995, 14, 5892– 5907
28. Santi, S.; Cesco, S.; Varanini, Z.; Pinton, R. Two plasma membrane H(+)-ATPase genes are differentially expressed in iron-deficient cucumber plants *Plant Physiol. Biochem.* 2005,43, 287– 292
29. Shen, H.; He, L. F.; Sasaki, T.; Yamamoto, Y.; Zheng, S. J.; Ligaba, A.; Yan, X. L.; Ahn, S. J.; Yamaguchi, M.; Sasakawa, H.; Matsumoto, H. Citrate secretion coupled with the modulation of soybean root tip under aluminum stress. Up-regulation of transcription, translation, and threonine-oriented phosphorylation of plasma membrane H+-ATPase*Plant Physiol.* 2005, 138, 287– 296
30. Gadd, G. M. Geomycology: biogeochemical transformations of rocks, minerals, metals and radionuclides by fungi, bioweathering and bioremediation *Mycol. Res.* 2007, 111, 3–49
31. Aust, A. E.; Lund, L. G.; Chao, C. C.; Park, S. H.; Fang, R. H. Role of iron in the cellular effects of asbestos *Inhalation Toxicol.* 2000, 12, 75– 80
32. Kamp, D. W.; Weitzman, S. A. The molecular basis of asbestos induced lung injury *Thorax*1999, 54, 638– 652
33. Lund, L. G.; Aust, A. E. Iron-catalyzed reactions may be responsible for the biochemical and biological effects of asbestos *Biofactors* 1991, 3, 83– 89
34. Du, J.; Gebicki, J. M. Proteins are major initial cell targets of hydroxyl free radicals *Int. J. Biochem. Cell Biol.* 2004, 36, 2334– 2343
35. Morel, M.; Kohler, A.; Martin, F.; Gelhaye, E.; Rouhier, N. Comparison of the thiol-dependent antioxidant systems in the ectomycorrhizal *Laccaria bicolor* and the saprotrophic *Phanerochaete chrysosporium New Phytol.* 2008, 180, 391– 407
36. Netto, L. E. S.; Chae, H. Z.; Kang, S. W.; Rhee, S. G.; Stadtman, E. R. Removal of hydrogen peroxide by thiol-specific antioxidant enzyme (TSA) is involved with its antioxidant properties—TSA possesses thiol peroxidase activity *J. Biol. Chem.* 1996, 271,15315– 15321
37. Zamocky, M.; Furtmüller, P. G.; Obinger, C. Evolution of catalases from bacteria to humans *Antioxid. Redox Signaling* 2008, 10, 1527– 1548
38. Tunc-Ozdemir, M.; Miller, G.; Song, L.; Kim, J.; Sodek, A.; Koussevitzky, S.; Misra, A. N.; Mittler, R.; Shintani, D. Thiamin confers enhanced tolerance to oxidative stress in*Arabidopsis Plant Physiol.* 2009, 151, 421– 432
39. Hohmann, S.; Meacock, P. A. Thiamin metabolism and thiamin diphosphate-dependent enzymes in the yeast *Saccharomyces cerevisiae*: genetic regulation *Biochim. Biophys. Acta* 1998, 1385, 201– 219
40. Ralser, M.; Wamelink, M.; Kowald, A.; Gerisch, B.; Heeren, G.; Struys, E.; Klipp, E.; Jakobs, C.; Breitenbach, M.; Lehrach, H.; Krobitsch, S. Dynamic rerouting of the carbohydrate flux is key to counteracting oxidative stress *J. Biol.* 2007, 6– 10
41. Yu, J. H.; Yun, S. Y.; Lim, J. W.; Kim, H.; Kim, K. H. Mass spectrometry and tandem mass spectrometry analysis of rat mitochondrial ATP synthase: up-regulation in pancreatic acinar cells treated with cerulein *Proteomics.* 2003, 3, 2437– 2445

42. Gaetani, G. F.; Galiano, S.; Canepa, L.; Ferraris, A. M.; Kirkman, H. N. Catalase and glutathione peroxidase are equally active in detoxification of hydrogen peroxide in human erythrocytes *Blood* 1989, 73, 334– 339
43. Riganti, C.; Aldieri, E.; Bergandi, L.; Fenoglio, I.; Costamagna, C.; Fubini, B.; Bosia, A.; Ghigo, D. Crocidolite asbestos inhibits pentose phosphate oxidative pathway and glucose 6-phosphate dehydrogenase activity in human lung epithelial cells *Free Radical Biol. Med.* 2002, 32, 938– 949